

IMPACT OF AIRFLOW ON THE THERMAL PERFORMANCE OF VARIOUS RESIDENTIAL WALL SYSTEMS UTILIZING A CALIBRATED HOT BOX

David C. Jones, P.E.
Member ASHRAE

ABSTRACT

A combination of ASTM E1424 and ASTM C976 was used to study the effect of airflow on thermal performance of various residential wall constructions. Typical residential 5.1-cm by 10.2-cm (2 by 4 nominal) and 5.1-cm by 15.4-cm (2 by 6 nominal) walls including a subfloor were covered with five types of exterior sheathing and different caulked joint arrangements either with or without a housewrap made from high-density flash spunbonded polyethylene. In the 34 different wall configurations, ASTM C976 tests were conducted at differential pressures of 0, 10, and 25 Pa per ASTM E1424. Airflows ranged from undetectable at 0 Pa ΔP to 1.63 L/s·m² (0.32 cfm/ft²) at 20 Pa. Thermal testing

results produced C-values from 0.49 to 0.30 W/m²·K (R-values of 3.29 to 2.05 K·m²/W) for a nondetectable airflow level to an effective C-value of 2.04 W/m²·K (effective R-value of 0.49 K·m²/W) for an airflow of 1.63 L/s·m². Tests on an "airtight drywall" (ADA) configuration were conducted to show the effect of "wind washing" on thermal performance, revealing that effective R-values decreased by 9% to 21% when exposed to wind pressures of 8 and 27 Pa vs. the wind pressure configuration of 0 Pa. These same ADA tests using a flash spunbonded polyethylene housewrap virtually eliminated the effective R-value loss due to "wind washing."

INTRODUCTION

The codes related to energy performance of residential walls in the United States, in their current state, have emphasized increased levels of mass insulation to affect overall energy-savings improvements. This is logical because it is relatively simple to calculate the energy-saving impact of adding additional R-value to a wall, and this can be backed up by measurements made in a lab under static conditions. The key word is *static*, or no air movement through or within the mass insulation. While testing under static conditions to establish an R-value levels the playing field for all forms of mass insulation, the results do not necessarily depict installed performance on a home.

Recent work done by Brown et al. (1993) illustrated the impact that slight defects in the installation of mineral fiber insulation would have on the overall system R-value of a wall. Earlier work done by Schuyler and Solvason (1983), Wolf et al. (1966), Berlad et al. (1979, 1982), and Lecompte (1987) all relates to loss in thermal performance due to convection within the wall cavity. Work by Henning (1983) illustrated the impact of air movement induced into the wall cavity on thermal performance using ASTM C-976, *Standard Test Method for*

Thermal Performance of Building Assemblies by Means of a Calibrated Hot Box (ASTM 1989). More recent work done by Ober and Goodrow (1994) and Jones et al. (1995) demonstrated that there was a significant impact on the thermal performance of a wall system from air infiltration with either mineral or cellulose insulation, and established a relationship for airflow rate through a wall and the associated impact on thermal performance at a fixed ΔT . This paper highlights the need to place a higher degree of emphasis on convective heat transfer in the overall thermal performance of a wall. Having adequate R-values for a wall is important; however, builders often fall short of understanding the need to go beyond achieving a particular R-value number and fail to introduce measures to reduce air infiltration.

EXPERIMENTAL DESIGN

To gain a further understanding of the impact of air leakage through a wall, 34 tests were conducted on 12 different wall configurations comparing the impact of using a housewrap vs. not. A flash spunbonded polyethylene housewrap was used on the wall configurations and exposed to a ΔT and varying exterior wind pressures. The 12 wall configurations consisted of six base wall assem-

David C. Jones is research associate at Tyvek® Market and Product Development at DuPont, Richmond, Va.

blies with and without the housetrap. Five of the wall assemblies were tested with a Δ pressure that induced full-penetration airflow through the wall, and one of the wall assemblies was tested with deadheaded wind pressure that did not fully penetrate through the wall. The apparatus used for these tests was a modified calibrated hot box that otherwise conforms to the requirements in ASTM C976 (the hot box included a guard chamber surrounding the metering chamber that afforded the ability to control the ambient temperature and pressure). Modifications are described in detail in the "Test Apparatus Description" section of this paper.

For each of six base wall assemblies, the first test configuration always tested a condition in which little or no airflow was permitted in or through the wall (static condition) by installing a 6-mil polyethylene film sheet over the entire exterior surface. Thermal testing was done at this static condition for each test configuration to ensure that no conditions had changed in the base wall assembly or operating equipment, because it would be expected that each of these test configurations would yield similar thermal performance under static conditions. After this first test, the polyethylene film was removed and, with the exception of tests 7 through 12, an air pressure differential was induced across the wall by pulling a vacuum inside the meter chamber. The suction side of a blower fan was connected to the meter chamber via flexible duct with a flowmeter in line to measure the airflow. The exhaust side of the blower fan was routed into the climate chamber (cold side of the hot box) to minimize the introduction of moist outside air into the system. A second blower fan was used to equalize the pressure between the guard chamber and the meter chamber to minimize any air exchanges that might occur at the meter chamber seal to the dividing wall. Pressure measurements were visually monitored using gauges and consistently maintained throughout each test.

After the last thermal test for each configuration grouping, but while there was still a temperature gradient across the wall, a pressure vs. air leakage test was performed conforming to ASTM E1424. The wall was then allowed to reach thermal equilibrium, where temperatures throughout the wall were the same and the air leakage test was repeated per ASTM E283.

Twenty-eight tests were performed on 10 different wall configurations with different static pressure differences across the sample with no measurable wind pressure on the cold side of the sample. The static pressure difference across the sample caused cold air to move through the wall assemblies, requiring additional heat input that was proportional to the infiltration rate. For each configuration, steady-state measurements of total heat flow, air infiltration rate, sample surface and internal temperatures, and localized heat flow (as measured by heat flux transducers) were made at test pressures of 0, 10, and 25 Pa or 0, 14.6, and 23.2 kph wind pressure. For tests

at zero pressure difference, the sample was covered with plastic on the exterior to prevent air infiltration from influencing the results. For subsequent tests at 10- and 25-Pa pressure difference, the plastic was removed to allow air to move through the sample. In addition to thermal measurements, air infiltration measurements at different wind pressures were made on each wall per ASTM Standard Test Method for Rate of Air Leakage Through Exterior Windows, Curtain Walls and Doors Under Specified Pressure and Temperature Differences Across the Specimen (E1424) (with a 21°C [70°F] temperature difference) and ASTM Standard Test Method for Rate of Air Leakage Through Exterior Windows, Curtain Walls and Doors (E283) (with no temperature difference at ambient conditions).

Tests 7 through 12 were designed to characterize the effect that "wind washing" might have on an "airtight drywall" installation. For these tests, the leakage locations on the warm side of the sample were sealed to simulate the "airtight drywall approach" (ADA). Using this approach, air was not allowed to flow through the wall, but it was possible for air to enter and exit the cold side of the sample through the seams in the exterior sheathing. This phenomenon, termed "wind washing," has been shown to affect the thermal performance of walls (Henning 1983; Jones et al. 1995). Wind pressure against a fixed wall will distribute pressure unevenly across the surface, causing areas of high and low pressure. Air infiltrates into the wall cavities at the higher pressure areas and exfiltrates through the same plane through the lower pressure areas. This air exchange carried heat away from the sample and increased the heat required to sustain a constant temperature on the warm side of the wall. The higher the wind pressure, the more air is forced into and out of the wall's interior and the higher the heat load becomes. To conduct these tests, a wind pressure was induced from the climate chamber's air circulation fans. The perpendicular airflow against the surface of the oriented strand board (OSB) sheathing was sufficient to produce areas of higher and lower pressure across the cold surface of the base wall assembly. Wind pressures equivalent to 12.9 and 24.1 kph (8 and 15 mph) or approximately 8 and 27 were measured at the surface of the OSB sheathing during the test by running a 0.64-cm (0.25-in.) plastic tube from that point to a gauge on the exterior of the chamber. Again, tests 7 and 10 were set up with the exterior polyethylene film to ensure static conditions and to provide a link to all of the other test configuration groupings. The exterior polyethylene film was removed for tests 8, 9, 11, and 12 and the wall was exposed to the potential for air exchange in and out from the same side. Airflow was monitored from the meter chamber throughout the test to ensure that no air penetration through the wall occurred. Tests 11 and 12 were designed to show the additive effect in thermal performance a housewrap might have on an "airtight drywall" installation. Air infiltration through

TABLE 1 Test Sample Configurations

Test	Description	Wind	
		Pa	Pressure kph
1	Nominal 2x4 Basewall Assy., foil faced pressure laminated cellulose sealed with plastic film	0	0
2	Test 1 without plastic film	10	14.6
3	Test 1 without plastic film	25	23.2
4	Test 1 with flash spunbonded PE Housewrap installed sealed with plastic film	0	0
5	Test 4 without plastic film	10	14.6
6	Test 4 without plastic film	25	23.2
7	Nominal 2x6 Basewall Assy. with OSB Sheathing and ADA sealed with plastic film	0	0
8	Test 7 without plastic film	8	12.9
9	Test 7 without plastic film	27	24.1
10	Test 7 with flash spunbonded PE Housewrap installed sealed with plastic film	0	0
11	Test 10 without plastic film	8	12.9
12	Test 10 without plastic film	27	24.1
13	Nominal 2x6 Basewall Assy. with hardboard siding under XPS Fanfold, vinyl and plastic film	0	0
14	Test 13 without plastic film	10	14.6
15	Test 13 without plastic film	25	23.2
16	Test 13 with flash spunbonded PE Housewrap between the XPS Fanfold and vinyl siding with film	0	0
17	Test 16 without plastic film	10	14.6
18	Test 16 without plastic film	25	23.2
19	Nominal 2x6 Basewall Assy. with 2 ft x 8 ft x 3/4 in. T&G XPS sealed with plastic film	0	0
20	Test 19 without plastic film	10	14.6
21	Test 19 without plastic film	20	20.8
22	Test 19 with flash spunbonded PE Housewrap over tongue and groove XPS sealed with plastic film	0	0
23	Test 22 without plastic film	10	14.6
24	Test 22 without plastic film	25	23.2
25	Nominal 2x6 Basewall Assy. with 4x8x1/2 in. foil faced polyisocyanurate foam sealed with plastic film	0	0
26	Test 25 without plastic film	10	14.6
27	Test 25 without plastic film	25	23.2
28	Test 25 with flash spunbonded PE Housewrap over foil faced polyisocyanurate foam without plastic film	10	14.6
29	Test 28 without plastic film	25	23.2
30	Test 25 with caulked sole plate/sub-floor interface sealed with plastic film	0	0
31	Test 30 without plastic film	10	14.6
32	Test 30 without plastic film	25	23.2
33	Test 30 with flash spunbonded PE Housewrap without plastic film	10	14.6
34	Test 30 with flash spunbonded PE Housewrap without plastic film	25	23.2

the sample was confirmed to be small, and the associated heat loss due to any infiltration was accounted for when calculating the sample heat flow. This is the case in normal C976 testing when air infiltration effects are minimized and factored out. Table 1 provides a brief description of all test configurations.

Previous testing (Jones et al. 1995) has shown that the exterior sheathing joints, coupled with interior seams and electrical penetrations in the drywall, are the primary flow paths of leakage. It also is apparent from this previous testing that the flash spunbonded polyethylene housewrap reduced air leakage to a somewhat predictable level regardless of the air leakage rate of the base wall without the housewrap. This is because the flash spunbonded polyethylene housewrap creates a consistent

level of air resistance. This paper expands on this point as it begins to explore the effects of using this housewrap with additional sheathing configurations.

TEST APPARATUS DESCRIPTION

Standard hot box testing per ASTM C976 does not include the effects of air infiltration, and samples are normally sealed to prevent air leakage from influencing the results. Because it was desired to incorporate air infiltration into this type of test, a calibrated hot box conforming to ASTM C976 was modified to introduce a pressure differential across the sample and a means of measuring air infiltration through the sample. These modifications provided a means of performing air infiltration tests on the

entire wall sample per ASTM E1424 and E283 in conjunction with the thermal tests. An additional modification (for tests with a static pressure difference only) to reduce the 24.1-kph (15-mph) equivalent wind pressure in the climatic chamber was done to minimize any air infiltration due to the associated dynamic pressure exerted on the sample. The air was circulated in the climatic chamber only enough to produce a uniform air temperature distribution, and the static pressure difference across the sample was achieved solely by blower fans in an external duct. For tests in which the wind was desired, air pressure measurements made near the sample surface with a pitot tube confirmed the wind pressure values desired, and air-flow measurements confirmed that air infiltration during these tests was small.

To minimize the potential for air and/or thermal leaks between the metering chamber and guard chambers, the two chambers were maintained at equal temperatures and pressures for all tests. Any small differences in temperature, and associated heat flows, were accounted for using methods described in ASTM C976.

BASE WALL DESCRIPTION

Except for different exterior sheathings, two base walls were tested. For the first six tests, a 2.44-m by 2.44-m (8-ft by 8-ft) base wall consisting of nominal 5.1-cm by 10.2-cm (2-in. by 4-in.) wood studs measuring 40.6 cm o.c. (16 in. o.c.) with a single bottom plate and double top plates was covered on the warm side with 1.3-cm (0.5-in.) gypsum board and was insulated with R-13 inset-stapled, kraft-faced fiberglass batts. A light switch on one side of the wall was wired to an outlet receptacle at the other end with a 14-gauge electrical service wire, thus connecting all of the stud cavities. Each stud had a 1.3-cm (0.5-in.) hole drilled through it to facilitate running the wire through the wall's interior. Extra care was taken to fit the insulation around the wire so as not to decrease the insulation thickness. Exterior sheathing for these first six tests was a 0.29 cm (0.113 in.) thick foil-faced, pressure-laminated cellulose. This base wall was placed on top of a 0.31-m by 2.44-m (1-ft by 8-ft) sub-floor with a band joist, floor joists measuring 40.6 cm (16 in.) o.c., 1.9-cm (0.75-in.) plywood sub-flooring, and R-13 insulation joist cavities.

For the next 28 tests, a second base wall was constructed that was similar to the first base wall except that it was framed with nominal 5.1-cm by 15.2-cm (2-in. by 6-in.) wood studs and insulated with R-19 inset-stapled, kraft-faced fiberglass batts. Also, each test series was conducted with a different exterior sheathing. The same sub-floor assembly was used throughout the entire testing program, with the exception that in tests 7 through 34, the R-13 insulation was replaced with an R-19 kraft-faced fiberglass batt.

Exterior siding was omitted in all but one test series (0.6-cm [0.25-in.] extruded polystyrene fan-folded leveling board) due to the difficulty in keeping this variable constant from test to test and also the wide variety of different sidings that are available. In the extruded polystyrene (XPS) fan-folded leveling board test series, siding was used because the siding is an integral part of that product's installation scheme. The usual installation of this product is for siding retrofit applications and involves installing it over "old" siding (usually wood) to provide a level surface for installing "new" siding (usually vinyl or aluminum) over it. Because the siding is not regarded as an air retarder, the perimeter of the siding was not sealed. However, the perimeter of the extruded polystyrene fan-folded leveling board, which is the intended air retarder in this system, was sealed to prevent air leakage between the leveling board and the sample frame.

The exterior sheathings used are described in Table 2. All the sheathings used in this testing program were installed following the manufacturer's suggested fastening schedule and installation instructions.

DETAILED TEST WALL DESCRIPTIONS

Tests 1 Through 6

The wall system for tests 1 through 6, illustrated in Figure 1, was a nominal 5.1-cm by 10.2-cm (2-in. by 4-in.) wood stud wall filled with R-2.27 m²·K/W (R-13 °F·ft²·h/Btu) inset-stapled kraft-faced fiberglass batts. The interior was sheathed with 1.27-cm (0.5-in.) gypsum drywall sealed around the perimeter and at the joint located horizontally approximately 1.22 m (4 ft) up from the subfloor assembly. A light switch and duplex receptacle were

TABLE 2 Test Wall and Sheathing Description

Test #	Framing	Sheathing
1 - 6	nominal 5.1 cm × 10.2 cm (2 in. × 4 in.)	Foil-faced pressure laminated cellulose (structural grade) 0.29 cm (0.113 in.) thick 1.22 m × 2.44 m (4 ft by 8 ft) sheets installed with 2.44 m dim. vertical)
7 - 12	nominal 5.1 cm × 15.2 cm (2 in. × 6 in.)	Oriented strand board 1.3 cm (1/2 in.) thick 1.22 m × 2.44 m (4 ft by 8 ft) sheets installed with 2.44 m dim. vertical)
13 - 18	nominal 5.1 cm × 15.2 cm (2 in. × 6 in.)	XPS fan-folded leveling board 0.6 cm (0.25 in.) thick 1.22 m × 2.44 m (4 ft by 8 ft) sheets installed with 2.44 m dim. vertical)
19 - 24	nominal 5.1 cm × 15.2 cm (2 in. × 6 in.)	XPS sheathing with tongue-and-groove joints 1.9 cm (3/4 in.) 0.61 m × 2.44 m (2 ft by 8 ft) sheets installed with 2.44 m dim. horizontal)
25 - 34	nominal 5.1 cm × 15.2 cm (2 in. × 6 in.)	Foil faced polyisocyanurate foam board 1.3 cm (1/2 in.) thick 1.22 m × 2.44 m (4 ft by 8 ft) sheets installed with 2.44 m dim. vertical)

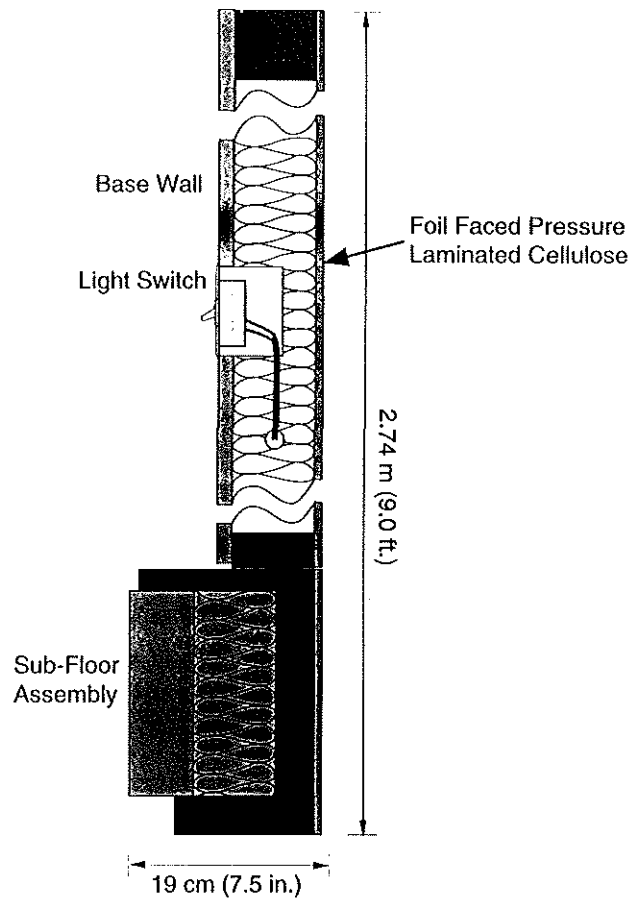


Figure 1 Tests 1 through 6 wall section.

installed as typical of residential construction with 1.27-cm (0.5-in.) holes drilled through each stud to run a standard 14-gauge wire between. The subfloor assembly was insulated with R-2.27 $\text{m}^2\cdot\text{K}/\text{W}$ (R-13 $^\circ\text{F}\cdot\text{ft}^2\cdot\text{h}/\text{Btu}$) kraft-faced fiberglass. Exterior sheathing was 1.22-m by 2.44-m (4-ft by 8-ft) foil-faced pressure-laminated cellulose (structural grade) approximately 0.29 cm (0.113 in.) thick installed with two 1.9-cm (0.75-in.) overlapping vertical joints across the 2.44-m (8-ft) wall width. (The manufacturer's instructions call for vertical joints to be overlapped but not horizontal joints.) The sheets were positioned at installation so that "manufactured edges" were present at all seams between joints. The sheathing was fastened with 3.2-cm (1.25-in.) roofing nails at 7.6-cm (3-in.) intervals around the perimeter and 15.2 cm (6 in.) along the intermediate studs. Air leakage points were identified at the sheathing joints on the exterior and at the baseboard area and electrical outlets on the interior.

Tests 7 Through 12

The wall system for tests 7 through 12, illustrated in Figure 2, was nominal 5.1-cm by 15.2-cm (2-in. by 6-in.) wood stud wall filled with R-3.33 $\text{m}^2\cdot\text{K}/\text{W}$ (R-19 $^\circ\text{F}\cdot\text{ft}^2\cdot\text{h}/\text{Btu}$) inset-stapled kraft-faced fiberglass batts. The interior was sheathed with 1/2-in. gypsum drywall

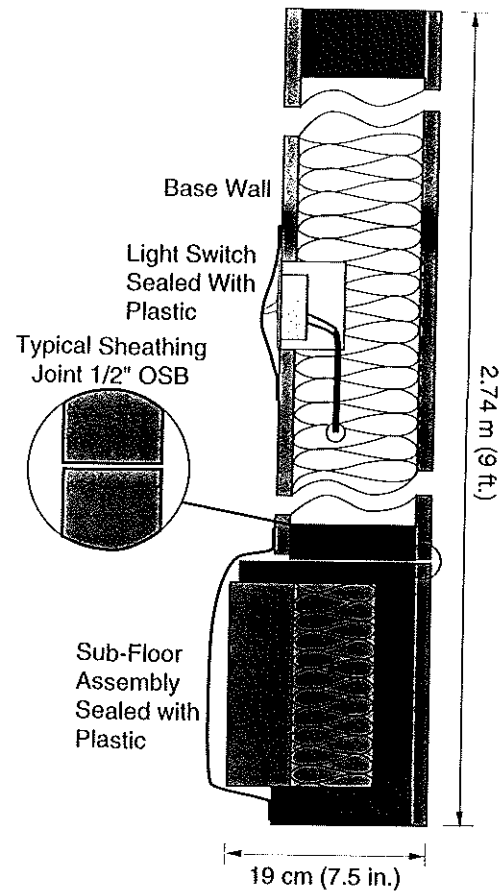


Figure 2 Tests 7 through 12 wall section.

sealed around the perimeter and at the joint located horizontally approximately 1.22 m (4 ft) up from the sub-floor assembly. A light switch and duplex receptacle were installed as typical of residential construction, with 1.27-cm (0.5-in.) holes drilled through each stud to run a standard 14-gauge wire between. The subfloor assembly was insulated with R-3.33 $\text{m}^2\cdot\text{K}/\text{W}$ (R-19 $^\circ\text{F}\cdot\text{ft}^2\cdot\text{h}/\text{Btu}$) kraft-faced fiberglass. Exterior sheathing was 1.22-m by 2.44-m by 1.3-cm (4-ft by 8-ft by 0.5-in.) oriented strand board installed with two vertical joints with 0.16-cm (0.0625-in.) gaps across the 2.44-m (8-ft) wall width. The sheathing was fastened with drywall screws at 30.5-cm (12-in.) intervals around the perimeter and 30.5 cm (12 in.) along the intermediate studs. The drywall side air leakage points at the baseboard area and through the electrical outlets were sealed with plastic and taped to simulate an airtight drywall installation. This wall was designed to allow no full-penetration air leakage; however, the joints in the exterior sheathing were not sealed, which could allow air to flow into the wall cavity and out along the same plane.

Tests 13 Through 18

The wall system for tests 13 through 18, illustrated in Figure 3, was identical to that used in tests 7 through 12 with

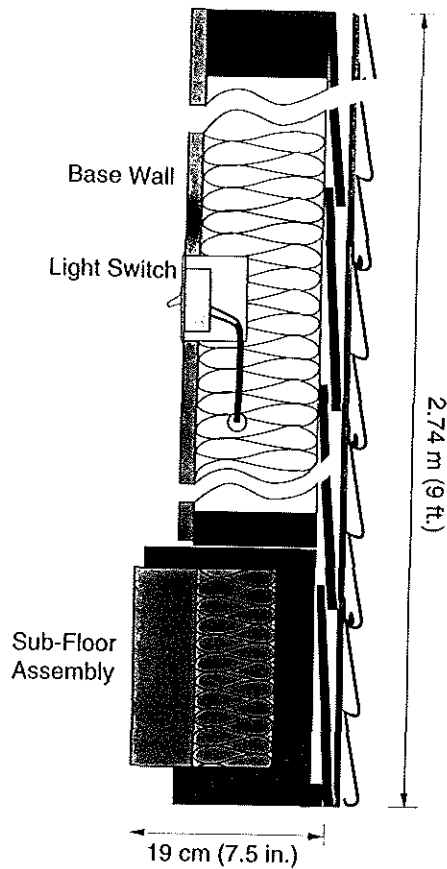


Figure 3 Tests 13 through 18 wall section.

the following changes: the plastic film was removed, which covered the interior electrical outlets and the subfloor assembly; and the 1.3-cm (0.5-in.) OSB sheathing was removed from the exterior. The exterior of the insulation cavity was covered with 30.5-cm (12-in.) hardboard siding followed by 0.6 cm (0.25 in.) thick fan-folded extruded polystyrene leveling board, and either a flash spunbonded polyethylene housewrap and type D4.5-22.9-cm (9-in.) vinyl siding or just type D4.5-22.9-cm (9-in.) vinyl siding without the flash spunbonded polyethylene housewrap. Both the 0.6-cm (0.2-in.) leveling board and the flash spunbonded polyethylene housewrap, if used, were sealed around the perimeter of the test wall. The 0.6-cm (0.25-in.) leveling board is supplied in 1.22-m (4-ft) widths, which rendered two horizontal seams along the 2.74-m (9-ft) height of the test wall. These seams were not sealed, which is typical of field installations. Air leakage points were identified at the seams in the leveling board on the exterior and at the baseboard area and electrical outlets on the interior.

Tests 19 Through 24

The wall system for tests 19 through 24, illustrated in Figure 4, was identical to that used in tests 7 through 12 with the following changes.

- The plastic film that covered the interior electrical outlets and the subfloor assembly was removed.

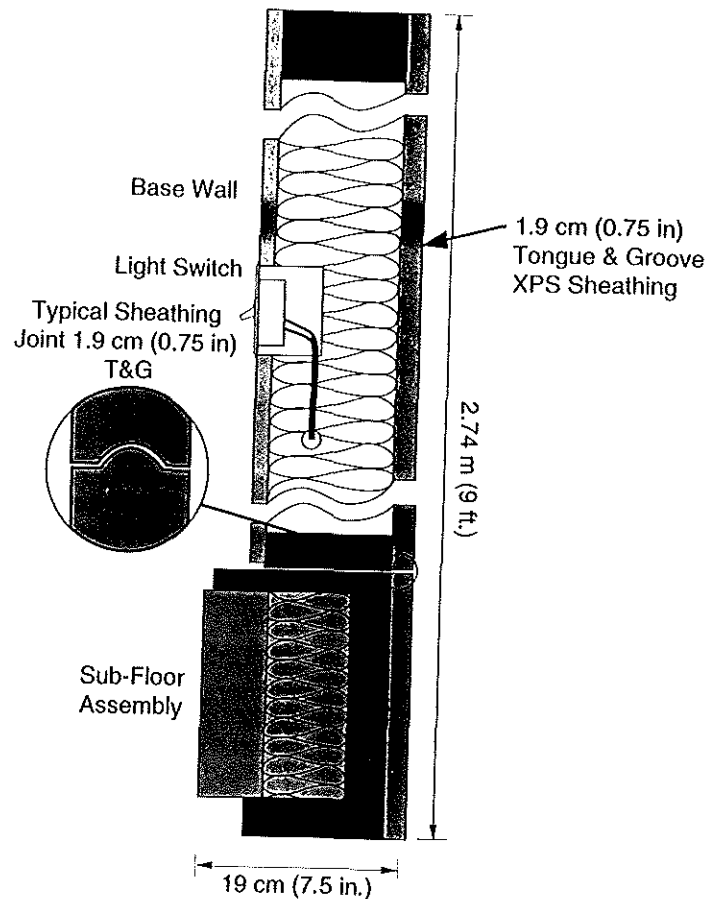


Figure 4 Tests 19 through 24 wall section.

- The 1.3-cm (0.5-in.) sheathing was removed from the exterior and replaced with 0.61-m by 2.44-m (2-ft by 8-ft) tongue-and-groove edged XPS sheathing because 1.22-m by 2.44-m (4-ft by 8-ft) sheets were not available in the vicinity of the testing facility. The tongue-and-groove XPS was installed horizontally per the manufacturer's installation schedule with 3.8 cm (1.5 in.) long drywall screws with 3.2-cm (1.25-in.) o.d. plastic washers. This installation created four 2.44-m (8-ft) horizontal seams and two 0.61-m (2-ft) vertical seams along a vertical stud. Pieces were fit together tightly using care to make sure all tongues and grooves were interlocked. The sheathing was fastened at 30.5-cm (12-in.) intervals along the vertical studs and 40.6 cm (16 in.) horizontally at each stud.

Air leakage points were identified at the sheathing joints on the exterior and at the baseboard area and electrical outlets on the interior.

Tests 25 Through 29

The wall system for tests 25 through 29, illustrated in Figure 5, was identical to that used in tests 7 through 12 with the following changes.

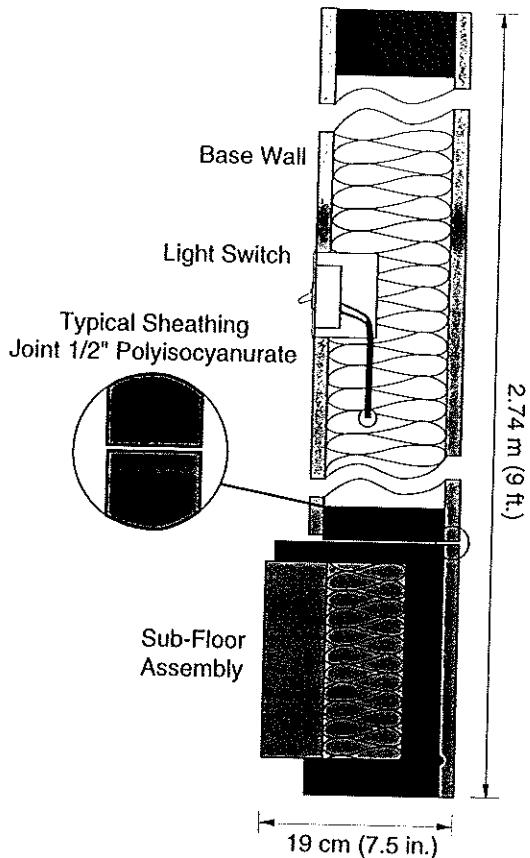


Figure 5 Tests 25 through 29 wall section.

- The plastic film that covered the interior electrical outlets and the subfloor assembly was removed.
- The 1.3-cm (0.5-in.) OSB sheathing was removed from the exterior and replaced with 1.22-m by 2.44-m by 1.3-cm (4-ft by 8-ft by 0.5-in.) square-edged foil-faced polyisocyanurate sheathing installed with two vertical joints across the 2.44-m (8-ft) wall width. The sheathing was fastened with drywall screws with washers at 30.5-cm (12-in.) intervals along the vertical studs and 40.6 cm (16 in.) horizontally at each stud.

Air leakage points were identified at the sheathing joints on the exterior and at the baseboard area and electrical outlets on the interior.

Tests 30 Through 34

The wall system for tests 30 through 34, illustrated in Figure 6, was identical to the wall configuration in tests 25 through 29 with the exception of added caulked joints at three locations. The purpose of these tests was to isolate the air leakage paths associated with the subfloor assembly. The interface between the subfloor and the bottom (sole) plate of the wall is a well-known leakage pathway. By applying caulk to this area to seal the path, which often is done just prior to tilting a wall in place, it is assumed that a major air leakage path is sealed. This test

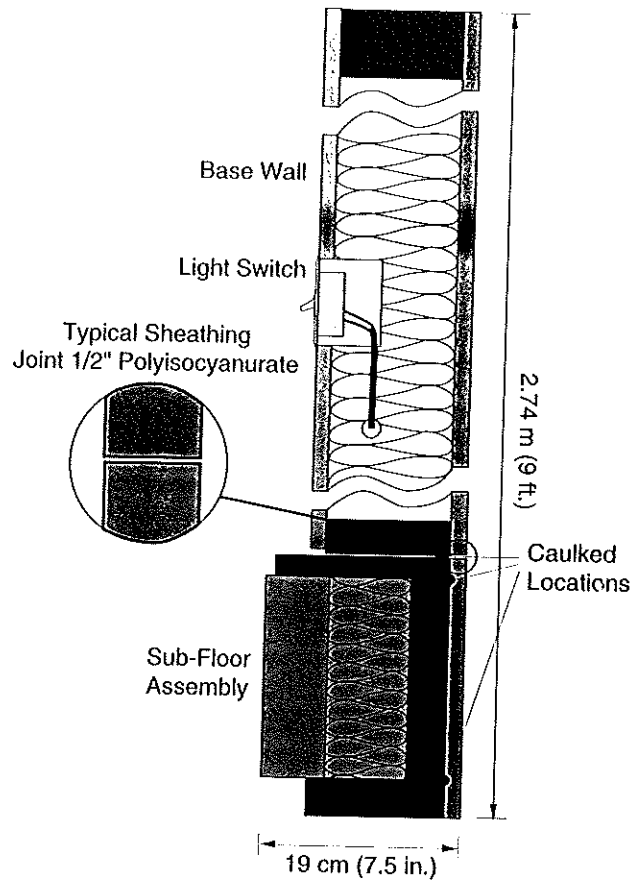


Figure 6 Tests 30 through 34 wall section.

was designed to gain a better understanding of the air leakage rates through the wall cavity when other air leakage pathways along the framing joints have been sealed. Air leakage points were identified at the sheathing joints on the exterior and at the electrical outlets and the baseboard area on the interior.

INSTRUMENTATION

Thermocouples used to measure temperatures during the tests were 24-gauge type-T with special limits of error. On each of the interior and exterior surfaces of the base wall, 16 thermocouples were installed as suggested in ASTM C976. These 32 thermocouples were placed at locations that were representative of the different conduction paths through the wall. Some were placed over studs, some were placed over insulation cavities, and others were placed at different locations on the subfloor area. The steady-state temperatures measured by these thermocouples were area-weighted in the final data analysis to provide an average sample surface temperature for both the warm and cold sides of the sample. These average surface temperatures defined the temperature gradients used in the effective conductance measurements for each test. The locations of these thermocouples did not change from sample to sample. An additional 48 thermo-

couples were located at various locations inside the wall and subfloor areas.

Thermocouples and heat flow transducer outputs were fed to a data-acquisition unit equipped with a 5½-digit voltmeter and an extension chassis with sufficient input cards to handle 220 channels. The voltmeter was calibrated using a National Institute of Standards and Technology (NIST)-traceable voltage source and has a manufacturer's stated accuracy of ±0.02% of reading +6μV for temperature measurements and ±0.016% of reading +360μV for power measurements. Actual calibration at the facility using a NIST-traceable voltage source showed that the accuracy was ±2μV total for temperature measurements and ±100μV total for power measurements. The data-acquisition unit was linked to a computer running software that monitored the test conditions. The software was set up to take data at five-minute intervals throughout the test and output to a text file that could later be analyzed and reduced using software for final output. Temperature control for each of the three chambers was accomplished by using controllers located within a hot box control console.

The heat flow into the metering chamber was computed as the sum of the power input to the heaters and the air-circulating fans. The heat (power) inputs were calculated using Equation 1:

$$P = V \cdot I \quad (1)$$

where

- P = power,
- V = volts, and
- I = amperage.

Voltage was measured by the voltmeter and current by measuring the voltage drop across a 0.01-ohm precision resistor that had been calibrated using a NIST-traceable resistor network. The heat input measurement provided the total heat flow, which, when corrected for other losses in the test apparatus, gave the heat flow through the sample.

Airflow was measured using one of three mass flowmeters providing the capability to measure airflows in three ranges: 0 to 0.5 L/s, 0 to 2.4 L/s, and 0 to 14.2 L/s (0 to 1 scfm, 0 to 5 scfm, and 0 to 30 scfm). Before each test, the appropriate flowmeter was selected so that leakage would fall as close as possible to the midrange of the measurement capability of the device. Each flowmeter had been calibrated with a NIST-traceable mass flowmeter and was accurate to ±3% of reading +0.5% of full scale.

Pressure was measured in the metering chamber using an indicating transmitter capable of sending a signal to the data-acquisition unit or being read visually by a dial indicator. Pressures in the climate chamber and guard chamber were measured by a pressure gauge that

was read visually. All of the pressure gauges were accurate to ±2% of full scale, which was 0 to 125 Pa (0 to 0.5 in. H₂O), and were readable in divisions of 2.5 Pa or 0.01 in. H₂O.

FACILITY CALIBRATION

Prior to the start of this testing program and again at its conclusion, a homogeneous wall of known R-value was run in the test facility. This wall was constructed of 10.2 cm (4 in.) thick expanded polystyrene foam faced with 0.32 cm (1/8 in.) thick plywood on both sides. Conductance measurements obtained per ASTM C518 in a NIST-traceable heat flowmeter apparatus were compared with the conductance measurements obtained in the hot box. The before and after R-value verification tests differed by 0.3%, and the average of the hot box runs differed from the ASTM C518 measured R-value by 0.1%.

SEALING TECHNIQUES AND VISUAL LEAKAGE CONFIRMATION

All sealing was done with the premise that air infiltration through the sample (through leakage pathways inherent in the construction techniques) was to be isolated and that air infiltration pathways created by the installation of the sample in the frame were to be eliminated.

To eliminate the air leakage between the sample and the sample frame in these tests, the base wall was sealed at the framing level all around the perimeter on both sides (warm and cold). On the warm side, the sample was again sealed all around the perimeter after the gypsum board was installed (the joint at the bottom plate of the wall and subfloor interface was not sealed in either instance). On the cold side, the sample was sealed again all around the perimeter after the exterior sheathing was installed.

For each wall configuration, the sample was checked for air leakage sites, using a smoke pencil, prior to the initiation of each test series. All perimeter sites were eliminated by sealing with tape and/or caulk. Leakage sites were confirmed for each sample to be at the electrical boxes and along the wall subfloor interface on the warm side, and along sheathing seams on the cold side. As was found in previous testing, leakage sites on the cold side of the sample along sheathing seams were much more pronounced between fasteners. Visual inspection confirmed a slight bowing of the sheathings, which explained this leakage. The bowing was characterized as the sheathing simply not being in contact with the stud frame (only in some locations), caused by the local deformation near the fasteners. The deformation was slight, and the only evidence of the sheathing not being in contact with the stud frame was felt when the sheathing was pushed on lightly. This phenomenon was more visually apparent with the foam sheathings, but smoke pencil checks confirmed leakage sites.

The OSB sheathing, the stiffest of the sheathings tested, did display some slight bowing away from the fastener locations, but the effect this had on the air leakage was not discernible because this sample was sealed on the warm side to simulate the "airtight drywall approach."

CALCULATED BASE WALL R-VALUES

Because each base wall configuration was tested with different sheathings, each test configuration had its own unique baseline R-value. This baseline establishes the "expected" wall thermal performance when there is no pressure difference across the wall. This thermal performance can then be compared to the thermal performance at different pressures to quantify the reduction in thermal performance due to air infiltration. This R-value was calculated for each wall using the parallel-path method based on verified conductance measurements for all wall components (per ASTM C518). The R-value for each wall also was measured (twice during each test series) in the hot box to confirm the validity of this calculation. Table 3 contains the calculated R- and C-values for the five wall assemblies. For all walls, this deviation (between "calculated" and "measured") was less than 5%.

TABLE 3 Calculated R- and C-Values for Test Wall Assemblies

Tests	Brief Description	Calculated	
		R-value m ² ·K/W	C-value W/m ² ·K
1 - 6	2 × 4 Foil faced pressure laminated cellulose (structural grade)	R-1.96	C-0.51
7 - 12	2 × 6 Oriented strand board	R-2.56	C-0.39
13 - 18	2 × 6 XPS fan folded leveling board	R-3.23	C-0.31
19 - 24	2 × 6 XPS sheathing with tongue and groove joints	R-3.33	C-0.30
25 - 34	2 × 6 Foil faced polyisocyanurate foam board	R-3.23	C-0.31

RESULTS

The results for the 34 tests are summarized in Tables 4 and 5. The relationship between air leakage through the wall and apparent thermal conductivity correlated well with previous testing (Jones et al. 1995). Figure 7 shows data from tests 13 through 34 from this current test and tests 1 through 28 from the work presented in Jones et al. (1995). Tests 13 through 34 were selected because the base walls all had similar calculated R-values at zero airflow (R-3.09 to R-3.29 m²·K/W or C-0.30 to C-0.32 W/m²·K). In tests 1 through 28 (Jones), the same basewall was used, which had a calculated R-value of R-2.5 m²·K/W or C-0.40 W/m²·K. In theory, these two plots should have produced parallel sloping lines, with the base walls with the higher R-values generating the lower of the two plots. Most of the data from tests 13 through 34 are positioned parallel and below the data from Jones et al. (1995) tests 1 through 2, with the exception of the data generated in test

Air Flow Rate vs. Apparent Thermal Conductance
Tests 13 - 34 and from Tests 1 - 28 Reference 9

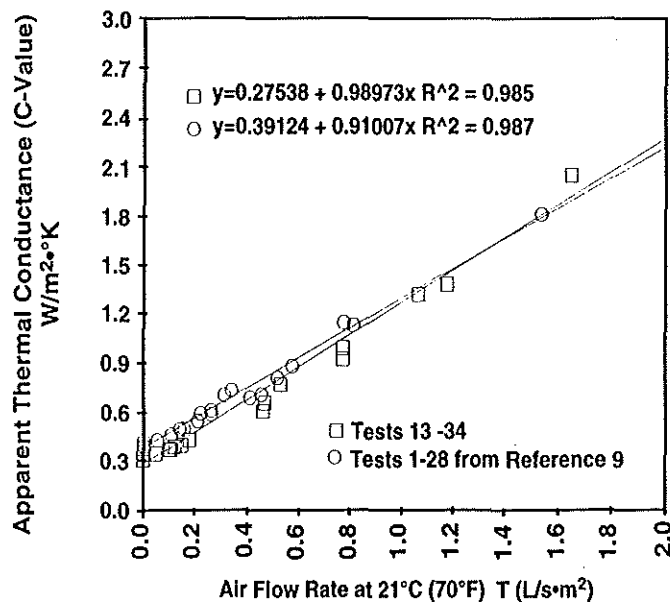


Figure 7 Comparison of airflow rate vs. effective thermal conductance for tests 13 through 34 and tests 1 through 28 from Jones et al. (1995).

21 (XPS tongue-groove), which had a greater loss in thermal performance than would be expected at the measured air leakage rate.

DISCUSSION

The presentation of these data presents an issue related to the dynamic nature from which it was generated. Because there was air movement at a steady state during the majority of the tests, the results cannot be presented as an R-value by its pure definition. However, the *ASHRAE Handbook of Fundamentals* (ASHRAE 1993a) does have a term—*apparent or effective thermal conductance* (C-factor or value)—that does allow for more than one mode of heat transfer through a sample. The units for C-value are W/m²·K. For static airflow conditions, ASHRAE provides definitions for R-value and U-factor that have units of K·m²/W and W/m²·K, respectively. U-factor and effective C-value share the same units, W/m²·K, separated only by the presence of an additional mode of heat transfer for effective C-value. There is, however, no corresponding term having the same units as R-value to express data that are generated with more than one mode of heat transfer. Because R-value is a widely used term in the industry, there should be a corresponding term, "effective ?-value," that would share the same units as R-value (K·m²/W) but cover the expression of data generated having more than one mode of heat transfer. For the purposes of presenting data in this paper, the author has decided to make the leap and express the data in

TABLE 4 Test Results

Test #	Description	Wind Speed	Heat Flow Rate		Effective C-Value		Effective R-Value	
		(kph)	(W)	(Btu/h)	(W/m ² ·K)	(Btu/h·ft ² ·°F)	(K·m ² /W)	(°F·h·ft ² /Btu)
1	Foil-faced pressure-laminated cellulose and plastic	0	109.16	372.57	0.49	0.09	2.05	11.63
2	Foil-faced pressure-laminated cellulose	14.6	309.29	1055.62	1.29	0.23	0.77	4.39
3	Foil-faced pressure-laminated cellulose	23.2	407.43	1390.57	1.71	0.30	0.58	3.32
4	Foil-faced pressure-laminated cellulose housewrap and plastic	0	109.01	372.05	0.49	0.09	2.06	11.68
5	Foil-faced pressure-laminated cellulose housewrap	14.6	126.45	431.57	0.53	0.09	1.87	10.64
6	Foil-faced pressure-laminated cellulose housewrap	23.2	131.57	449.05	0.55	0.10	1.81	10.29
7	2x6 OSB ADA	0	94.34	321.97	0.41	0.07	2.47	14.01
8	2x6 OSB ADA	12.9	110.64	377.60	0.44	0.08	2.26	12.83
9	2x6 OSB ADA	24.1	128.56	438.77	0.52	0.09	1.94	11.00
10	2x6 OSB ADA, housewrap, plastic	0	92.38	315.30	0.39	0.07	2.54	14.43
11	2x6 OSB ADA, housewrap	12.9	93.16	317.95	0.38	0.07	2.55	14.77
12	2x6 OSB ADA, housewrap	24.1	91.69	312.95	0.38	0.07	2.65	15.05
13	XPS Fan fold leveling board and plastic	0	77.35	263.99	0.32	0.06	3.14	17.85
14	XPS Fan fold leveling board	14.6	152.17	519.36	0.61	0.11	1.63	9.27
15	XPS Fan fold leveling board	23.2	226.41	772.73	0.92	0.16	1.08	6.15
16	XPS Fan fold leveling board, housewrap, plastic	0	77.72	265.26	0.31	0.05	3.24	18.42
17	XPS Fan fold leveling board and housewrap	14.6	92.71	316.41	0.37	0.07	2.71	15.38
18	XPS Fan fold leveling board and housewrap	23.2	108.12	369.03	0.43	0.08	2.32	13.17
19	3/4 in. XPS T&G and plastic	0	76.88	262.38	0.31	0.06	3.20	18.18
20	3/4 in. XPS T&G	14.6	327.12	1116.46	1.38	0.24	0.73	4.12
21	3/4 in. XPS T&G	20.8*	474.84	1620.62	2.04	0.36	0.49	2.78
22	3/4 in. XPS T&G, housewrap, and plastic	0	74.77	255.19	0.30	0.05	3.29	18.69
23	3/4 in. XPS T&G and housewrap	14.6	87.36	298.17	0.35	0.06	2.85	16.17
24	3/4 in. XPS T&G and housewrap	23.2	98.38	335.77	0.40	0.07	2.52	14.34
25	Foil-faced isocyanurate and plastic	0	77.22	263.56	0.32	0.06	3.11	17.65
26	Foil-faced isocyanurate	14.6	189.09	645.38	0.77	0.14	1.30	7.36
27	Foil-faced isocyanurate	23.2	317.64	1084.12	1.32	0.23	0.76	4.29
28	Foil-faced isocyanurate and housewrap	14.6	87.03	297.02	0.35	0.06	2.83	16.05
29	Foil-faced isocyanurate and housewrap	23.2	93.77	320.03	0.38	0.07	2.63	14.93
30	Foil-faced isocyanurate caulked	0	76.84	262.27	0.32	0.06	3.09	17.54
31	Foil-faced isocyanurate caulked	14.6	163.03	556.41	0.66	0.12	1.51	8.55
32	Foil-faced isocyanurate caulked	23.2	240.18	819.73	0.99	0.18	1.01	5.71
33	Foil-faced isocyanurate, housewrap and caulked	14.6	87.45	298.46	0.36	0.06	2.81	15.95
34	Foil-faced isocyanurate, housewrap and caulked	23.2	96.94	330.86	0.39	0.07	2.54	14.41

*The samples leakage rate exceeded the capacity of the blower and did not permit this test to be conducted at the desired 23.2 kph wind pressure.

terms of effective C-value and effective R-value, fully acknowledging that there is no current referenceable definition for effective R-value. For this paper, effective R-value will use the units of K·m²/W and be the reciprocal of effective C-value.

The test design does not incorporate any exterior siding, which would be an additional variable that might contribute to the thermal performance of a wall. Because

there are a multitude of different exterior sidings, it would be impossible to characterize them all with this type of test protocol. Furthermore, residential exterior sidings are not typically considered to function as an air retarder, although in some cases there may be some contribution. The level of sealing detail that would be required to make a bevel-lapped siding airtight, for instance, would be cost prohibitive and the longevity of the seal, if achieved,

TABLE 5 Air Leakage Rates

Test #	Description	Wind Speed (kph)	Air Leakage ASTM E1424		Air Leakage ASTM E283	
			(cfm/ft ²)	(L/s·m ²)	(cfm/ft ²)	(L/s·m ²)
1	Foil faced pressure laminated cellulose and Plastic	0	0	0	0	0
2	Foil faced pressure laminated cellulose	14.6	0.15	0.76	0.11	0.56
3	Foil faced pressure laminated cellulose	23.2	0.23	1.18	0.19	0.97
4	Foil faced pressure laminated cellulose Housewrap and Plastic	0	0	0	0	0
5	Foil faced pressure laminated cellulose Housewrap	14.6	0.01	0.04	0.01	0.04
6	Foil faced pressure laminated cellulose Housewrap	23.2	0.02	0.08	0.01	0.06
7	2x6 OSB ADA	0	0	0	0	0
8	2x6 OSB ADA	12.9	0	0	0	0
9	2x6 OSB ADA	24.1	0	0	0	0
10	2x6 OSB ADA, Housewrap, Plastic	0	0	0	0	0
11	2x6 OSB ADA, Housewrap	12.9	0	0	0	0
12	2x6 OSB ADA, Housewrap	24.1	0	0	0	0
13	XPS Fan fold leveling board and Plastic	0	0	0	0	0
14	XPS Fan fold leveling board	14.6	0.09	0.45	0.06	0.30
15	XPS Fan fold leveling board	23.2	0.15	0.76	0.13	0.66
16	XPS Fan fold leveling board, Housewrap, Plastic	0	0	0	0	0
17	XPS Fan fold leveling board, and Housewrap	14.6	0.02	0.10	0.01	0.05
18	XPS Fan fold leveling board, and Housewrap	23.2	0.03	0.17	0.02	0.10
19	3/4 in. XPS T&G and Plastic	0	0	0	0	0
20	3/4 in. XPS T&G	14.6	0.23	1.16	0.13	0.66
21	3/4 in. XPS T&G	20.8*	0.32	1.63	0.23	1.17
22	3/4 in. XPS T&G, Housewrap, and Plastic	0	0	0	0	0
23	3/4 in. XPS T&G and Housewrap	9.1	0.02	0.08	0.01	0.05
24	3/4 in. XPS T&G and Housewrap	23.2	0.03	0.14	0.01	0.05
25	Foil Faced Isocyanurate and Plastic	0	0	0	0	0
26	Foil Faced Isocyanurate	14.6	0.10	0.52	0.05	0.25
27	Foil Faced Isocyanurate	23.2	0.21	1.05	0.11	0.56
28	Foil Faced Isocyanurate and Housewrap	14.6	0.01	0.05	0.01	0.05
29	Foil Faced Isocyanurate and Housewrap	23.2	0.02	0.09	0.01	0.05
30	Foil Faced Isocyanurate Caulked	0	0	0	0	0
31	Foil Faced Isocyanurate Caulked	14.6	0.09	0.46	0.05	0.25
32	Foil Faced Isocyanurate Caulked	23.2	0.15	0.76	0.10	0.51
33	Foil Faced Isocyanurate, Housewrap and Caulked	14.6	0.01	0.05	0.01	0.05
34	Foil Faced Isocyanurate, Housewrap and Caulked	23.2	0.02	0.11	0.01	0.05

*The samples leakage rate exceeded the capacity of the blower and did not permit this test to be conducted at the desired 23.2 kph wind pressure.

would be questionable with continual contraction and expansion of the siding as moisture content varies.

The selection of 10- and 25-Pa pressure difference used throughout the tests is slightly higher than average U.S. wind conditions, which range from roughly 8 to 16 kph (5 to 10 mph) (GRI 1992). These wind conditions vary seasonally and with geographic region and, obviously, as the wind speed decreases, the impact of pressure-induced convective heat losses decreases. Buildings also can be inadvertently pressurized and depressurized by imbalances in heating, ventilating, and air-conditioning (HVAC) systems that can induce infiltration or exfiltration through exterior walls if sufficient resistance to airflow is not built in. It is not suggested, however, that use of a housewrap or other air retarder in an exterior wall would be a good substitute for correcting imbalances in an HVAC system.

The ability to compute actual energy savings for a given building based on results from this testing is not possible due to the many variables that impact thermal performance under actual conditions. However, it is these same variables that also introduce inaccuracies in energy modeling based on static thermal performances of materials and systems. The testing has been conducted to illustrate the vulnerability of some insulating materials to air movement and to make the point that a statically measured R-value is only as good as the ability to maintain that static condition in actual use. The test results consistently illustrate the value of installing a flash spunbonded housewrap for reducing air movement in walls whose insulation performance is sensitive to air movement.

The foil-faced, pressure-laminated, cellulose-sheathed walls (tests 1 through 3) had a significant decrease in effective R-value (increase in effective C-value) as the Δ pressure was increased due to increased airflow through the wall assembly. A large amount of this air leakage occurred through the subfloor/sole plate interface and through the electrical boxes. When a flash spunbonded polyethylene housewrap was applied in tests 4 through 6, the rate of heat loss was significantly reduced for the same Δ pressures due to reduced airflow through the wall assembly. For a 14.6-kph (9.1-mph) wind pressure, the foil-faced, pressure-laminated, cellulose-sheathed wall wrapped with a flash spunbonded polyethylene housewrap only allowed the effective R-value to drop about 9% vs. 62% for just the sheathing without housewrap. At 23.5 kph (14.4 mph), the effective R-value with a flash spunbonded polyethylene housewrap dropped about 12% vs. about 71% for just the sheathing without housewrap.

Data for the OSB configuration (using the "airtight drywall approach") showed that the effective R-value of the sample is adversely affected by the effects of "wind washing." At a wind pressure of 12.9 kph (8 mph) blowing against the exterior of the wall, the effective R-value decreased by about 9% even though no air actually penetrated completely through the wall. At 24.1-kph (15-mph) wind pressure, the effective R-value decreased by about 21%. Consequently, when a flash spunbonded polyethylene housewrap was wrapped over the exterior of these walls, no decrease in effective R-value for both the 12.9- and 24.1-kph (8- and 15-mph) wind speeds was noted. A slight increase in effective R-value was measured as wind pressure was increased when the flash spunbonded polyethylene housewrap was used, which cannot be explained. It should not be concluded from these data that the wall's thermal performance would improve beyond that measured at static conditions if wind pressure is induced. The installation of a flash spunbonded polyethylene housewrap did, however, effectively eliminated the negative effects of "wind washing."

Data for the XPS fan-folded leveling board and tongue-and-groove configurations showed that these products are not very effective in reducing air infiltration. The air infiltration rate of these products also exhibited a sensitivity to temperature. That is, the air infiltration rate at a given pressure was higher when a temperature difference existed across the sample (see Table 5). The XPS fan-folded leveling board also has many tiny holes poked through its surface and these holes may expand and contract with changing temperatures. For the XPS fan-folded leveling board wall assembly, the equivalent wind pressures of 14.6 and 23.5 kph (9.1 and 14.4 mph) decreased the effective R-value by about 48% and 66%, respectively. When a flash spunbonded polyethylene housewrap was wrapped over these test walls, the effective R-value

decreased about 16% and 28% for the same wind pressure conditions. For the XPS tongue-and-groove wall assembly, the increased air infiltration rate at lower temperatures is presumably due to the interlocking nature of the product. These products both rely on interlocking seams as barriers to air infiltration, and, as they cool, the coefficient of thermal expansion may cause sufficient movement to reduce the sealing nature of the interlocking seams. At 9.1- and 12.9-mph equivalent wind pressure, the XPS tongue-and-groove sheathing allowed sufficient air leakage to decrease the effective R-value by about 77% and 85%, respectively. When a flash spunbonded polyethylene housewrap was wrapped over these test walls, the effective R-value only decreased 13% and 23% for the same wind pressure conditions.

Data for the foil-faced polyisocyanurate sheathing configuration showed that caulking the leakage sites in the subfloor area was successful in reducing air infiltration, but only by a small percentage vs. no caulking. Comparing tests 25 and 26 with tests 30 and 31 shows that at 14.6-kph (9.1-mph) equivalent wind pressure the effective R-value was only increased 7% by caulking the interface between the subfloor and the sole plate. The overall loss in effective R-value was about 58% without caulking and 51% with caulking at 14.6-kph (9.1-mph) equivalent wind pressure. With or without caulking, wrapping with a flash spunbonded polyethylene housewrap at a 14.6-kph (9.1-mph) equivalent wind pressure only allowed a 9% loss in effective R-value. It was speculated, prior to this testing, that the interface between the subfloor and the sole plate was the main source of air leakage in the wall assembly. While this interface does constitute a major leakage site, sealing it only changes the path of least resistance through the wall assembly. The results from tests 25 through 34 clearly show that significant amounts of air can penetrate into the wall cavity at the bottom horizontal interface between the exterior sheathing and the sole plate (Figure 8) even though the interface between the sole plate and the sub-floor is sealed. For this configuration, the air exits the wall on the interior side through the electrical boxes and at the horizontal joint between the drywall and the sub-floor. Previous testing documented in Ober and Goodrow (1994) of work conducted for a manufacturers' association indicates that little air penetrates into the wall cavity and out through electrical box penetrations in the interior drywall. Although there were some similarities between the organization's test configurations and the work presented in this paper, there are a couple of important differences.

- The organization's wall did not include the sub-floor section and was sealed around the perimeter, allowing air to flow into the wall only at the two vertical seams in the exterior sheathing and out through the electrical boxes on the interior side.
- The organization's wall did include exterior siding (which is not considered to be an air barrier but may

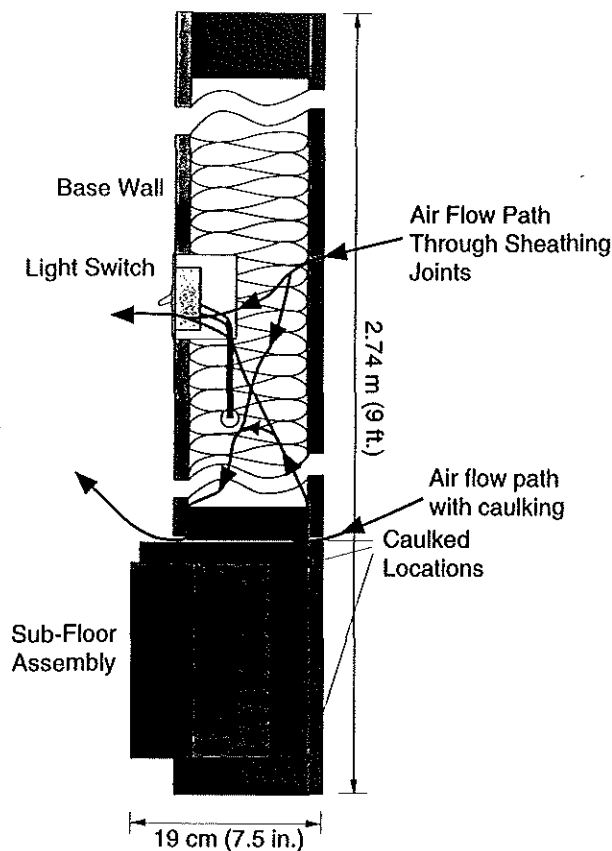


Figure 8 Airflow paths through the foil-faced polyisocyanurate wall assembly used for tests 25 through 34.

impact the air leakage characteristics of the wall assembly).

It would be inappropriate to attempt to quantify air leakage associated with a particular pathway by integrating the data from Ober's tests with this testing due to dissimilarities in the test samples.

The foil-faced polyisocyanurate wall, like the XPS fan-folded leveling board and tongue-and-groove walls, showed a sensitivity to temperature gradient across the wall. The air infiltration rates (Table 5) were significantly higher for walls with a temperature gradient than for walls without a temperature gradient. This may be due to a higher propensity for joint movement due to thermal expansion and possibly the differential in thermal expansion between the foil and the polyisocyanurate foam.

CONCLUSIONS

The flash spunbonded polyethylene housewrap was effective in significantly reducing the air infiltration rates for all configurations tested. It also was effective in reducing the effects of "wind washing," based on data gathered in the "airtight drywall approach" tests. For tests with air infiltration, the flash spunbonded polyethylene housewrap reduced the air infiltration rates in the same range as

was previously documented in Jones et al. (1995). These results show that this housewrap is effective in reducing air infiltration to predictable levels. This level is in the range of 0.001 to 0.003 L/s·m² (0.015 to 0.03 cfm/ft²) at 25-Pa pressure and is somewhat independent of the air infiltration rate of the wall without the housewrap. The air infiltration rate of walls with a flash spunbonded polyethylene housewrap is slightly affected by temperature gradient across the wall but only when the wall without the housewrap is significantly affected by the same temperature gradient. This would indicate that there is a synergistic effect between all wall components in establishing the air-retarding performance of a wall system. The use of the term "effective R-value" was used in this paper, although no definition currently exists in the *ASHRAE Handbook of Fundamentals* (ASHRAE 1993a). There is a need for this type of term to be added to the definitions in chapter 20 since, intuitively, R-value expresses thermal performance in terms where bigger numbers mean better performance. Since there is an "effective C-value," there should also be a reciprocal. The findings of this paper also suggest that there should be continued emphasis placed on reducing air exchanges through the building envelope by various practices such as using a housewrap in the language of ASHRAE Standard 90.2 (ASHRAE 1993b) and in the CABO Model Energy Code (CABO 1995).

ACKNOWLEDGMENTS

The author wishes to recognize the considerable assistance in test design and execution from John T. Goodrow working at Holometrix Inc., Bedford, Mass.

REFERENCES

- ASHRAE. 1993a. 1993 ASHRAE handbook—Fundamentals, p. 20.1. Atlanta, Ga.: American Society of Heating, Refrigerating and Air-Conditioning Engineers, Inc.
- ASHRAE. 1993b. ASHRAE Standard 90.2-1993, Energy-efficient design of new low-rise residential buildings. Atlanta, Ga.: American Society of Heating, Refrigerating and Air-Conditioning Engineers, Inc.
- ASTM. 1989. ASTM Standard C-976, Standard test method for thermal performance of building assemblies by means of a calibrated hot box. Philadelphia, Pa.: American Society for Testing and Materials.
- Berlad, A.L., N. Tutu, R. Jaung, and Y.-J. Yeh. 1979. Energy transport in porous insulator systems. ORNL/Sub-7551/1. Oak Ridge, Tenn.: Oak Ridge National Laboratory.
- Berlad, A.L., R. Jaung, N. Joshi, and J. Westerinen. 1982. Energy transport in porous insulator systems. ORNL/Sub-7551/2. Oak Ridge, Tenn.: Oak Ridge National Laboratory.
- Brown, W.C., M.T. Bomberg, and J.M. Ullett, J.M. 1993. Measured thermal resistance of frame walls with defects in the installation of mineral fibre insulation. *Journal of Thermal Insulation and Building Environments* 16 : 318-339.
- CABO. 1995. 1995 CABO model energy code. Falls Church, Va.: Council of American Building Officials.
- GRI. 1992. *The weather almanac*, 6th ed., F.E. Bair, ed. Gale Research Inc.
- Henning, G.N. 1983. ASTM STP 789, Energy conservation with air infiltration barriers. *Thermal insulation, materials, and*

- systems for energy conservation in the '80s*, F.A. Govan, D.M. Greason, and J.D. McAllister, eds., pp. 551-558. Philadelphia, Pa.: American Society for Testing and Materials.
- Jones, D.C., D.G. Ober, and J.T. Goodrow. 1995. Thermal performance characterization of residential wall systems utilizing a calibrated hot box with air flow induced by differential pressures. In *ASTM STP 1255, Air Flow Performance of Building Envelopes, Components, and Systems*, M.P. Modera and A.K. Persily, eds., pp. 197-228. Philadelphia, Pa.: American Society of Testing and Materials.
- Lecompte, J.G.N. 1987. The influence of natural convection in an insulation cavity on thermal performance of a wall. *Insulation Materials Testing and Applications*. Philadelphia, Pa.: American Society of Testing and Materials.
- Ober, D.G., and J.T. Goodrow. 1994. Effect of cavity insulation, vapor retarders, and air retarders on air infiltration of residential walls. *Proceedings of the 12th Annual International Energy Efficient Buildings Conference and Exposition*, Dallas, Texas, February 23-26.
- Schuyler, G.D., and K.R. Solvason. 1983. Effectiveness of wall insulation. In *ASTM STP 789, Thermal Insulation, Materials, and Systems for Energy Conservation in the '80s*, F.A. Govan, D.M. Greason, and J.D. McAllister, eds., pp. 542-550. Philadelphia, Pa.: American Society of Testing and Materials.
- Wolf, S., K.R. Solvason, and A.G. Wilson. 1966. Convective air flow effects with mineral wool circulation in wood-framed walls. *ASHRAE Transactions* 72(II): III 3.1-III 3.8.